THE ANATOMICAL RECORD 298:29–47 (2015)

Form and Function in the Platyrrhine Skull: A Three-Dimensional Analysis of Dental and TMJ Morphology

CLAIRE E. TERHUNE,[1]* SIOBHÁN B. COOKE,[2,3]
AND ERIK OTÁROLA-CASTILLO[4,5]
[1]Department of Anthropology, University of Arkansas, Fayetteville, Arkansas
[2]Department of Anthropology, Northeastern Illinois University, Chicago, Illinois
[3]New York Consortium in Evolutionary Primatology Morphometrics Group, New York, New York
[4]Department of Ecology, Evolution, and Organismal Biology, Iowa State University, Ames, Iowa
[5]Department of Human Evolutionary Biology, Harvard University, Cambridge, Massachusetts

ABSTRACT

Cranial and temporomandibular joint (TMJ) form has been shown to reflect masticatory forces and mandibular range of motion, which vary in relation to feeding strategy. Similarly, the dentition, as the portion of the masticatory apparatus most directly involved in triturating food items, strongly reflects dietary profile. Fine control over condylar and mandibular movements guides the teeth into occlusion, while the topography and position of the dental arcade mediate mandibular movements. We hypothesize that masticatory, and particularly TMJ, morphology and dental form covary in predictable ways with one another and with diet. We employed three-dimensional geometric morphometric techniques to examine inter-specific variation in ten platyrrhine species. Landmarks were collected on six datasets describing the upper and lower molars, cranium, glenoid fossa, mandible, and mandibular condyle; two-block partial least squares analyses were performed to assess covariation between cranial morphology, dentition, and diet. Significant relationships were identified between the molars and the cranium, mandible, and glenoid fossa. Some of these shape complexes reflect feeding strategy; for example, higher crowned/cusped dentitions, as found in primates consuming larger quantities of structural carbohydrates (e.g., *Alouatta* and *Saimiri*), correspond to anteroposterior longer and deeper glenoid fossae. These results indicate strong covariance between dental and TMJ form, aspects of which are related to feeding behavior. However, other aspects of morphological variation display a strong phylogenetic signal; we must therefore examine further ways in which to control for phylogeny when examining covariation in interspecific masticatory form. Anat Rec, 298:29–47, 2015. © 2014 Wiley Periodicals, Inc.

Key words: dietary adaptation; dentition; masticatory apparatus; geometric morphometrics

---

Additional Supporting Information may be found in the online version of this article.

Grant sponsor: National Science Foundation; Grant numbers: NSF BCS-0752661, NSF DDIG 40761-0001, NSF 0333415, NSF (BCS-0923791); Grant sponsor: National Evolutionary Synthesis Center; Grant number: NSF EF-0905606; Grant sponsor: Leakey Foundation.

*Correspondence to: Claire E. Terhune, Department of Anthropology, University of Arkansas, Fayetteville, AR 72701. E-mail: cterhune@uark.edu

Received 3 October 2014; Accepted 11 October 2014.

DOI 10.1002/ar.23062

Analyses of morphological variation typically focus on restricted regions of anatomy with the goal of quantifying variation across a group of specimens or species and linking this variation with behavioral or functional differences among taxa. This approach is critical for understanding the range of morphological variation, and often helps with the development of new hypotheses that can be tested experimentally. The atomization of morphological variation in this way is often borne out of necessity: the inclusion of fragmentary fossils may require the region of analysis be circumscribed; the morphology of other regions may be difficult to quantify; or the scope of the analysis simply does not permit a broader study.

The masticatory apparatus provides a case in point. Although the many components of the masticatory apparatus act as a single functional unit, the majority of analyses focus on specific subregions of anatomy such as the teeth, mandible, or the temporomandibular joint (TMJ) (e.g., Kay, 1975; Rosenberger and Kinzey, 1976; Hylander, 1979; Cooke, 2011; Terhune, 2011a). But while dental morphology has been tightly linked to feeding strategy (e.g., Kay, 1975, 1978, 1984; Rosenberger and Kinzey, 1976; Anapol and Lee, 1994; M'Kirera and Ungar, 2003; Ungar and M'Kirera, 2003; Evans et al., 2007; Cooke, 2011), the bony morphology of the skull has typically been considered a less reliable indicator of diet, while still reflecting forces related to chewing (e.g., Taylor 2002, 2005; Norconk et al., 2009; Terhune, 2011a; Ross et al., 2012). However, the degree of covariation in the shape of these two components of the masticatory apparatus has not been previously evaluated. Here, we suggest that evaluating covariation between these two datasets and linking this covariation to dietary profile will provide a more integrative understanding of diet-related morphology. We focus specifically on covariation in platyrrhine primates as a test case.

Evidence Linking Dental Form and Diet

Across primates, the dentition, as the portion of the masticatory apparatus that is most directly involved in triturating food items, has been shown to strongly reflect dietary regimes (e.g., Kay, 1975; Rosenberger and Kinzey, 1976; Anapol and Lee, 1994; Boyer, 2008; Cooke, 2011). Primates specializing in foods including structural carbohydrate tend to have more complex molar teeth with greater shearing capabilities, and in some cases higher crowns to resist wear, than primates specializing in soft fruit or seeds. Leaves are generally better digested when sheared into smaller pieces, which creates more surface area upon which digestive acids, bacteria, and enzymes can act (Stevens and Hume, 1995). Consequently, platyrrhines such as *Alouatta*—a large-bodied semi-folivorous form—have relatively large teeth for their body size, longer shearing crests, and higher crowns than other platyrrhines of equal mass (Kay, 1975; Anapol and Lee, 1994; Rosenberger et al., 2011).

Insectivorous primates also tend to have specialized dentition, with a significant puncture-crushing component to mastication. In some analyses of dental morphology using measures of shear, there is significant overlap between insectivorous forms consuming chitinous insects and folivorous forms if body size is not included (e.g., Kay, 1975). However, the type of insects consumed (chitinous vs. non-chitinous) also influences morphology. Amongst the cebids, the squirrel monkey, *Saimiri*, primarily prefers grasshoppers and other chitinous forms, while *Cebus capucinus*, the capuchin monkey, specializes in softer bodied organisms such as caterpillars as well as harder nuts and fruits. These feeding differences may explain the lack of a substantial degree of shear in *Cebus* molar morphology (Janson and Boinski, 1992; Tomblin and Cranford, 1994).

Among mostly frugivorous taxa, the dentition tends toward having relatively shorter shearing crests. Behaviorally, these primates focus on "pulping" fruits before swallowing. Consequently, measures of dental form in these taxa show expanded crushing basins and a moderate degree of shear (Kay and Hiiemae, 1974; Kay, 1975). Finally, primates such as the pitheciine seed predators and some species of *Cebus* habitually consume hard fruits and nuts and show few adaptations to shearing food items. The pitheciines in particular have wide basins and crenulated enamel (Ledogar et al., 2013) and primarily process hard seeds through substantial crushing force. In addition to having dental morphologies adapted to breaking down hard food items, they also possess decussated enamel, which makes their dentition particularly resistant to fracture (Martin et al., 2003).

While biologists have observed for centuries that dental morphology reflects an animal's diet (e.g., Owen, 1840; Osborne, 1907; Gregory, 1922; Simpson, 1933), it is only since the 1970s that methodologies developed to quantify and capture more complex morphological differences have been employed in biological anthropological analyses. Kay and Hiiemae (1974) identified and characterized dental morphologies responsible for crushing, grinding, and shearing on primate molar teeth and correlated these measures with differences in diet and jaw movement. This work was subsequently expanded with the development of Kay et al.'s Shearing Quotient (SQ) (Kay, 1978; Kay and Hylander, 1978; and Kay and Covert, 1984), a measure of a tooth's relative ability to shear a food item. In addition to the highly influential SQ, a number of three-dimensional measures of surface complexity (orientation patch count) and relief have shown some success in separating primates by dietary category (e.g., Ungar and Williamson, 2000; M'Kirera and Ungar, 2003; Ungar and M'Kirera, 2003; Evans et al., 2007; Boyer, 2008; Winchester et al., 2014). All of these methods work on the principle that plant food must be broken down to a greater extent than animal-based foods for efficient digestion. One way of accomplishing this is by increasing the length of shearing blades, but an animal can also pack more fracture sites into the tooth crown by increasing the complexity of the surface such that with each occlusal stroke more food is fractured.

Evidence Linking Cranial Form and Diet

Like the dentition, variation in bony morphology of the cranium and mandible has also been linked to differences in feeding behavior among primate taxa. However, the relationship between diet and bony morphology tends to be less straightforward, and studies provide conflicting results. Perhaps the strongest link between skull morphology and diet is exhibited by variation in the position of the muscle resultant force relative to the bite force; decreasing this lever-to-load arm ratio converts more muscle force to bite force. Resistant object feeders therefore tend to exhibit either a shorter distance from the TMJ to the bite point, and/or a muscle resultant positioned closer to the bite point; notably these morphological configurations also function to decrease the joint reaction force (e.g., Herring and Herring, 1974; Ward and Molnar, 1980; Greaves, 1980; Spencer, 1995, 1999; Wright, 2005; Constantino, 2007). Similarly, resistant object feeders tend to have TMJs situated higher above the occlusal plane (e.g., Spencer, 1995; Taylor, 2002; Constantino, 2007; Terhune, 2011b). By positioning the TMJ in this way the attachment area and moment arms of the masticatory muscles are increased (Maynard Smith and Savage, 1959; Greaves, 1974; DuBrul, 1977; Freeman, 1988; Spencer, 1995) and/or forces are more evenly distributed along the postcanine dentition (Herring and Herring, 1974; Greaves, 1980; Ward and Molnar, 1980; Spencer, 1995).

The dimensions of the mandibular symphysis and corpus also vary in relation to dietary demands. The more folivorous colobines exhibit deeper and wider corpora and symphyses relative to the more frugivorous cercopithecines (Hylander, 1979; Bouvier, 1986a; Ravosa, 1990), and within cercopithecines deeper corpora are also found in hard-object eating mangabeys (e.g., Hylander, 1979; Bouvier, 1986a). In the African apes, corpus and symphysis robusticity reflect degree of folivory, with the most folivorous apes (*Gorilla beringei*) possessing relatively larger symphyses and corpora than less folivorous gorillas and chimpanzees (Taylor, 2002, 2006). However, it is notable that these patterns of shape differences are not necessarily consistent across clades; although platyrrhine seed predators (e.g., *Chiropotes*) exhibit relatively more robust corpora, platyrrhine folivores such as *Alouatta* do not (Bouvier, 1986a). Furthermore, analyses of mandibular cross-sectional geometry have provided little support for a linkage between internal mandibular architecture and diet, suggesting instead that perhaps the mandible is overdesigned (Daegling, 1989, 2007).

Features of the TMJ have also been linked to feeding behavior in primates (Smith et al., 1983; Bouvier, 1986a,b; Wall, 1995, 1999; Vinyard, 1999; Vinyard et al., 2003; Taylor, 2005; Terhune, 2011a,b, 2013). On the basis of the scaling analyses of the mandibular condyle, Smith et al. (1983) and Bouvier (1986a,b) suggested that condylar dimensions were larger in taxa that exploited more resistant food items, and mediolateral width of the condyle has been linked to increased twisting of the mandibular corpus as occurs during cyclical loading of the mandible (Hylander, 1979; Hylander and Bays, 1979; Bouvier, 1986a,b). Experimental analyses also suggest that condylar dimensions should vary in relation to joint loading, as condylar dimensions are significantly larger in both rats and rabbits fed relatively more resistant diets (e.g., Bouvier and Hylander, 1984; Ravosa et al., 2008). However, subsequent analyses have yielded few consistent patterns in condylar dimensions among extant primates (Taylor, 2005, 2006; Terhune, 2011a, 2013). Notably, these analyses have done little to successfully differentiate among tough and hard object feeders. Furthermore, substantially more TMJ features can be securely linked to differences in mandibular range of motion than to inferred joint loading. For example, taxa that employ feeding or social behaviors that necessitate large gapes have relatively anteroposteriorly longer joint surfaces (both of the glenoid fossa and condyle), and this relationship appears to hold true within strepsirrhines (Vinyard et al., 2003), platyrrhines (Wall, 1995, 1999; Vinyard et al., 2003; Terhune, 2011a), and catarrhines (Wall, 1995, 1999; Terhune et al., 2011; Terhune, 2013).

Covariance Between Dental and Cranial Form

Although the above studies suggest that dental form can be linked to diet, it is important to note that dental form does not necessarily reflect the most frequently consumed food items, since these foods may not necessarily exert as much selective pressure on the dentition as other less frequently consumed, but highly important foods (Kay, 1975; Rosenberger and Kinzey, 1976; Anapol and Lee, 1994). Anapol and Lee (1994) found that molar morphology in platyrrhine primates was most suited to processing important sources of protein (e.g., insects or leaves). For example, *Saimiri*, the squirrel monkey, consumes large quantities of easily processed fruit, but during certain low fruiting times of the year can have a diet made up of 80% insects and other prey (Lima and Ferrari, 2003). Here, the critical function of the dentition would be geared toward mastication of insects even though insects are not the most frequently consumed food item for large parts of the year.

Similarly, the results of the above outlined work on bony morphology suggest that although the exploitation of resistant food items is typically accompanied by particular cranial forms, the utilization of tough (e.g., leaves) and hard (e.g., seeds) food items may exert different selective pressures over masticatory form through different mandibular loading regimes. The exploitation of tough foods such as leaves (which are generally low in quality) is often accompanied by cyclical loading of the mandible but this repetitive loading may be at relatively low peak magnitudes, whereas hard food items, once breached, are typically brittle and may therefore only require a few bites at very high magnitudes (e.g., Hylander, 1984, 1985; Williams et al., 2007, 2009). At present, it is unclear how we might proceed with inferring these two distinct loading regimes based solely on the bony morphology of the mandible. However, given the comparatively well-documented and direct relationship between dental morphology and hard versus tough food items (i.e., crushing vs. shearing), coupling bony morphology and dental morphology may allow us to more easily distinguish between morphologies linked to these different adaptive strategies.

Biomechanically, there are a number of reasons we might expect dental and cranial form (and especially the morphology of the TMJ) to be tightly linked. Fine control over condylar and mandibular movements (whether via bony or soft tissue structures) guides the teeth into occlusion during the fast close phase of the gape cycle (Hiiemae, 1978; Hiiemae and Crompton, 1985), at which point the teeth are prepared to come into occlusion, as occurs during the slow close phase. Critically, the power stroke, when teeth are in direct contact with the food item and/or each other, occurs during the transition from the slow close to slow open portions of the gape cycle. The power stroke itself can be broken down into two distinct components: phase I and phase II movements (Kay and Hiiemae, 1974). On the active side, phase I begins when the lower molars attain a lateral position relative to the upper molars and continues as they move anteromedially into occlusion when the protocone enters the talonid basin. The anteromedial movement continues, and phase II begins as the molars drop downward and move out of occlusion.

Mandibular movements during the power stroke are primarily mediolateral (i.e., lateral deviation), where the balancing-side (i.e., non-chewing) condyle translates anteriorly, medially, and inferiorly along the articular eminence and the working-side (i.e., chewing) condyle translates only slightly anteriorly and shifts laterally. Experimental studies of mandibular movement suggest that lateral deviation increases with increased resistance of the food item (Byrd et al., 1978; Anderson et al., 2002; Komiyama et al., 2003; Wall et al., 2006; but see Reed and Ross, 2010). These movements should, in theory, be governed both by the form of the TMJ and by the pattern of dental occlusion produced by dental topography. As the teeth come out of occlusion and the slow open phase of the gape cycle begins, the mandibular condyle glides and rotates freely anteriorly along the cranial articular surface of the TMJ (aka, glenoid or mandibular fossa) and the condyle moves anteriorly and inferiorly along the slope of the articular eminence (AE). Increases in the amount of lateral deviation should be accompanied by increased translation of the balancing side condyle and increased mediolateral shifting of the working side condyle.

Morphological Predictions

Despite this biomechanical framework, it is unclear exactly how we might expect dental and TMJ morphology to covary, as no studies have systematically examined covariance between these two systems. Furthermore, we generally lack solid experimental data quantifying the exact nature of mandibular, and hence dental and condylar, movements during non-human primate masticatory behaviors. The few kinematic data available (e.g., Wall, 1999; Terhune et al., 2011; Iriarte-Diaz et al., in preparation), preliminarily suggest patterns of mandibular movement are highly idiosyncratic, but species specific differences in mandibular movement do occur (Iriarte-Diaz et al., 2013).

One previous hypothesis linking dental and masticatory form was posited by Hylander (1979, 1988), who suggested that the flat occlusal profile of robust australopiths (i.e., *Paranthropus*) allowed for an increase in the lateral component of the bite force. These increased lateral movements would in turn have resulted in increased twisting of the mandibular corpus that must be countered by buccolingually broader symphyses and corpora. Conversely, Hylander hypothesized that primates with high crowned teeth (e.g., colobines) experience relatively less transverse and anterior mandibular movements because of the precise nature in which the teeth must come into occlusion. Therefore these taxa possess relatively deep mandibles to counteract the sagittal bending moments produced by these forces.

On the basis of this previous hypothesis by Hylander, we propose several ways in which dental and skull form—particularly that of the TMJ—may covary in platyrrhine primates:

H1: The precise nature of occlusion in animals that emphasize vertical shear during food processing, should mean that they experience relatively less mandibular lateral deviation during mastication. Thus, we predict that dental morphologies optimized for shearing (i.e., high crowned and cusped teeth) will covary with glenoid morphologies that constrain lateral deviation [i.e., mediolaterally narrow joints (Hylander 1979; Bouvier, 1986a,b) with large entoglenoid processes (Wall, 1999)].

H2: In animals that emphasize crushing-grinding during food processing (i.e., fruit and seed consumers), lateral deviation should be relatively high so that the lateral component of the bite force is increased. We therefore predict that dental morphologies optimized for crushing (i.e., bunodont dentitions) will covary with TMJ morphologies that facilitate mandibular lateral deviation [i.e., mediolaterally wide condyles and glenoids (Hylander, 1979; Bouvier, 1986a,b), and small entoglenoid processes (Wall, 1999)].

We test these hypotheses here using three-dimensional (3D) geometric morphometric (GM) techniques designed to capture and analyze the overall shape of the masticatory apparatus and the dentition with an aim toward attaining a greater understanding of the functional morphology of this anatomical region. While the data presented in this study do not include experimental evidence for jaw movement, these analyses will help to generate hypotheses that can be tested experimentally. We examine this covariation in a sample of platyrrhine primates. This clade provides an excellent test case, as they are a diverse monophyletic radiation with species of many different body sizes belonging to many dietary guilds.

MATERIALS AND METHODS

Sample

Our sample included representatives of males and females from all three platyrrhine primate families (Fig. 1). Samples were drawn from the collections of the American Museum of Natural History and the Smithsonian Institution's National Museum of Natural History. Body sizes ranged from approximately 1 kg (*Saimiri*) to nearly 10 kg (*Ateles*) (Ford and Davis, 1992), and the sample included primates specializing in a variety of different food types including soft fruit specialists (*Ateles, Lagothrix*), seed predators (*Pithecia*, *Chiropotes*, *Cacajao*), frugivore-insectivores (*Saimiri*) and semi-folivorous forms (*Alouatta*). Dietary data for *Aotus* are scant, but it is generally considered a soft-fruit frugivore. While genera, and in most cases, species, sampled in the cranio-mandibular and dental datasets overlap, no individuals overlapped in the two datasets; consequently, covariation seen between the datasets represents a low-end estimate of what might exist in analyses of data from the same individuals. For two genera, *Saimiri* and *Aotus*, different species were sampled. The cranio-mandibular datasets includes *Saimiri sciureus* and *Aotus trivirgatus*, and the dental dataset includes *S. boliviensis* and a combined dataset of several different species of *Aotus* including *A. trivirgatus, A. infulatus, A. vociferans*, and *A. lemurinus*. Dentally, the *Aotus* species are not distinct. All individuals chosen for analysis were non-pathological and dentally adult.

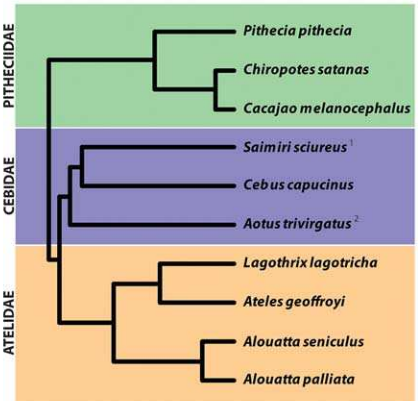

	Cranium and Glenoid	Mandible and Condyle	Upper Molar	Lower Molar
Pithecia pithecia	11/10	11/12	2/4	2/4
Chiropotes satanas	11/11	12/12	8/6	8/6
Cacajao melanocephalus	8/14	8/14	4/4	4/4
Saimiri sciureus[1]	10/5	10/10	12/17	11/17
Cebus capucinus	13/11	13/11	13/13	12/13
Aotus trivirgatus[2]	11/10	11/10	19/11	18/10
Lagothrix lagotricha	11/11	10/12	7/5	7/5
Ateles geoffroyi	12/11	13/12	8/8	8/5
Alouatta seniculus	11/10	12/12	5/5	4/4
Alouatta palliata	11/10	12/12	8/8	7/7

Fig. 1. Consensus tree with branch lengths (downloaded from 10Ktrees.fas.harvard.edu; version 3; Arnold et al., 2010) and table showing sample sizes for each dataset. Values represent number of females followed by the number of males (females/males). [1]The cranial and mandibular samples for this species are from *Saimiri sciureus*, while the dental data are for *Saimiri boliviensis*. [2]The cranial and mandibular samples for this species are from *Aotus trivirgatus*, while the dental data are an aggregate of specimens from *A. trivirgatus, A. infulatus, A. vociferans*, and *A. lemurinus*.

Data Collection

Three-dimensional *x,y,z* coordinate landmarks on the cranium and mandible were chosen to capture aspects of masticatory, facial, and basicranial morphology (Table 1, Fig. 2). The cranial landmarks were captured by CET using a Microscribe G2X digitizer (Immersion Corp.). Error for the Microscribe G2X is ±0.23 mm, and analysis of intraobserver error in the dataset from which these samples were drawn (Terhune, 2010) identified an average error for the skull of ~0.03 and 0.04 mm for the mandible.

Dental data were collected by SBC on epoxy casts, created using methods outlined in Cooke (2011), of unworn upper and lower second molars. Specimens were rejected if the cusp tips showed exposed dentin or substantial flattening. All casts were laser scanned using an LDI Surveyor AM-66RR laser scanner with an RPS 120 sensor at 25 μm interpoint distances to create three-dimensional models of tooth rows. Individual second molars were cropped from the tooth row using Geomagic Studio 11 (Geomagic). Landmark data (Table 2, Fig. 3) were then collected using Landmark Editor (Wiley et al., 2005). The landmark set was developed to outline the major features of the molar occlusal surface including cusp tips, basin low points, and crest intersections as well as features of tooth sidewalls (Table 2, Fig. 3). The intraobserver error for landmark placement was found to be significantly lower than interspecific variation (Cooke, 2011).

Data Analysis

Six separate datasets were created from the mixed-sex landmark data: upper molar, lower molar, cranium and glenoid, glenoid only, mandible and condyle, and condyle only. Analyses where males and females were analyzed separately were qualitatively similar to the combined sex sample. For each of the six datasets, we performed a series of analyses in the program R (*R* Development Core Team, 2008) using the package "geomorph" (Adams and Otárola-Castillo, 2013). First, mean forms for each species were calculated and superimposed using generalized procrustes analysis (GPA). We then examined the extent to which a phylogenetic signal was present in each of the datasets by calculating the sum of squared changes in shape along the branches of a consensus phylogeny downloaded from 10Ktrees.fas.harvard.edu (Arnold et al., 2010; phylogeny shown in Fig. 1). Statistical significance of this signal was assessed by performing a permutation test (9,999 iterations) where shape data were shuffled among the tips of the phylogenetic tree. The phylogenetic signal was then visualized by overlaying the consensus tree on a plot of the first two axes of a principal component analysis (PCA).

We examined the role of allometry in each of the datasets by performing multivariate regressions of the Procrustes aligned coordinates ("shape") on size. Two size variables were employed: the natural log of the centroid size of the configurations under examination, and the natural log of mandibular length (as a measure of the load arm during incisal behaviors). Mean mandibular length for each species was calculated as the linear distance between the midpoint of the articular surface of the condyle (Table 1, landmark M9) and infradentale (Table 1, landmark M2). These regressions were performed with and without a consideration of phylogenetic covariation. To account for phylogenetic autocorrelation we estimated the models' parameters using Phylogenetic Generalized Least Squares (PGLS; detailed in Grafen, 1989; Garland and Ives, 2000; Rohlf, 2001), which accounts for the effects of sampling from closely related species on the regression model. In this study, we assumed a Brownian motion model of evolution, and we employed a consensus phylogenetic tree that was downloaded from 10Ktrees.fas.harvard.edu (Arnold et al., 2010) (Fig. 1). These PGLS regressions allowed us to extract regression residuals for each dataset that were adjusted for size and phylogeny; these regression residuals were then employed in all subsequent analyses. We evaluated the significance of both the non-PGLS and PGLS regression models by permuting the Procrustes distances among specimens and calculating the sum-of-squared Procrustes distances (Goodall, 1991). The empirical distribution of the permuted sum-of-squared Procrustes distances was then used to evaluate if the original observed sum-of-squared Procrustes distances were extreme. We performed this permutation test using 9,999 iterations.

To assess whether our dental and cranial datasets covaried with diet, we compiled published data reporting the percentage of fruit, leaves, seeds (where reported separately), and insects consumed by each species (Table 3). We visualized this dietary matrix by performing an unweighted pair group average (UPGMA) cluster analysis, which allowed us to compare this 'diet tree' to the phylogeny. We then examined the relationship between each of the dental and cranial datasets and the dietary matrix using two-block partial least squares (PLS) analysis (Rohlf and Corti, 2000). Two-block PLS [also referred to as a singular warps analysis; Bookstein et al.

TABLE 1. Cranial and mandibular landmarks employed in this study

Subset	Landmark #	Landmark description
Cranium	1	Prosthion
	2	Nasospinale
	3	Nasion
	4	Glabella
	5	Bregma
	6	Basion
	7	Midpoint of sphenooccipital synchondrosis
	8	Hormion
	9	Intersection of median and transverse palatine sutures
	10	Point on alveolar margin at the midpoint of maxillary P4
	11	Point on alveolar margin at the midpoint of maxillary M1
	12	Point on alveolar margin at the midpoint of maxillary M2
	13	Point just posterior to the alveolus of the last maxillary molar
	14	Orbitale
	15	Opposite side orbitale
	16	Maxillofrontale
	17	Frontomolare orbitale
	18	Point where temporal line and coronal suture meet
	19	Jugale
	20	Point on the superior border of the zygomatico-temporal suture
	21	Most posterior point on margin of temporal fossa in sagittal plane
	22	Most anterior point on cranial masseteric scar
	23	Most lateral point on anterior basicranium at the spheno-occipital synchondrosis
	24	Most lateral point on posterior basicranium / most medial point on jugular fossa
	25	Point at intersection of infratemporal crest and sphenotemporal suture
	26	Most lateral point on foramen ovale
	27	Apex of the petrous
	28	Most inferolateral point on the carotid canal
	29	Most inferior point on the tympanic plate/tube in the coronal plane of porion
	30	Porion
	31	Opposite side porion
	32	Asterion
	33[a]	Most inferior point on entoglenoid process
	34[a]	Most inferior point on articular tubercle
	35[a]	Most inferior point on postglenoid process
	36[a]	Deepest point in mandibular fossa in sagittal plane of PGP point
	37[a]	Most anterior point on the articular surface of the glenoid fossa
	38[a]	Most lateral point on articular surface of glenoid at end of long axis of AE
	39[a]	Most lateral point on surface of articular eminence
	40[a]	Most medial point on surface of articular eminence
	41[a]	Most medial point on articular surface of glenoid at end of long axis of AE
	42[a]	Midpoint of crest of articular eminence
	43[a]	Most anterior point on articular surface of glenoid along line perpendicular to the long axis of the AE
	44[a]	Point on posterior edge of AE along line perp to long axis of AE
Mandible	M1	Gnathion
	M2	Infradentale
	M3	Most inferior point on mental foramen
	M4	Point on alveolar margin at the midpoint of mandibular P4
	M5	Point on alveolar margin at the midpoint of mandibular M1
	M6	Point on alveolar margin at the midpoint of mandibular M2
	M7[b]	Most lateral point on articular surface of condyle
	M8[b]	Most medial point on articular surface of condyle
	M9[b]	Midpoint of line connecting medial and lateral poles of condyle
	M10[b]	Most posterior point on articular surface of condyle at midpoint of ML curve
	M11[b]	Most anterior point on mandibular condyle at midpoint of ML curve

[a] Landmarks used in the glenoid only analysis.
[b] Landmarks used in the condyle only analysis.

(2003)] is an appropriate method to employ here because it does not assume that one dataset is dependent upon the other. Here we present the PLS correlation between the first singular warp axes for each dataset along with the RV coefficients (Klingenberg, 2009) describing the overall relationship between the two blocks of data, and we visualize the relationship between each of the first singular warp axes for each dataset through a bivariate plot of the PLS scores. All of these PLS analyses were performed using the phylogeny and size adjusted regression residuals. We present results only for those regressions that employed mandibular length as the size

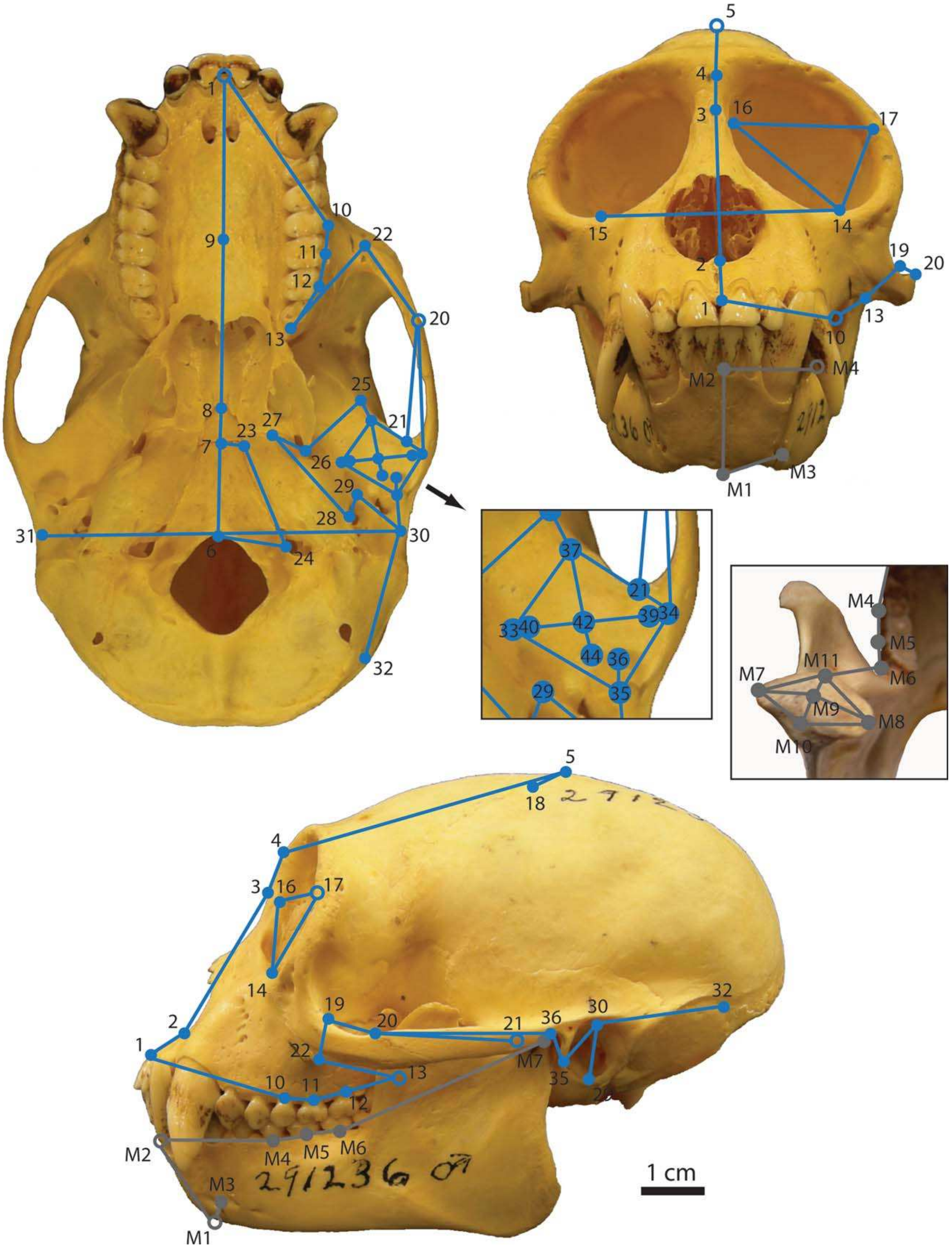

Fig. 2. Inferior (left), anterior (top right), and lateral (bottom) views of an adult male *Cebus capucinus* skull showing the cranial (blue) and mandibular (gray) landmarks and wireframes employed in this study. Insets in middle of figure show close-ups of the glenoid fossa (left) and mandibular condyle (right). Landmark numbers correspond to those listed in Table 1.

TABLE 2. Dental landmarks employed in this study

Subset	Landmark #	Landmark description
Madibular M_2	1	Metaconid apex
	2	Protoconid apex
	3	Hypoconid apex
	4	Entoconid apex
	5	Mesial-most point on occlusal surface
	6	Distal-most point on occlusal surface
	7	Lowest point on the protocristid - usually at the midline
	8	Lowest point on the cristid obliquid
	9	Point at which the preentocristid and postmetacristid meet
	10	Lowest point in the trigonid basin
	11	Lowest point in the talonid basin
	12	Point of maximum curvature directly below the protoconid
	13	Point of intersection of the ectoflexid with the buccal wall
	14	Point of maximum curvature directly below the hypoconid
	15	The cemento-enamel junction (CEJ) directly below the protoconid
	16	Point on the CEJ directly below the intersection of the ectoflexid with the buccal wall
	17	Point on the CEJ directly below the hypoconid
	18	Point of maximum curvature directly below the entoconid
	19	Point of maximum curvature directly below where the preentocristid and postmetacristid meet
	20	Point of maximum curvature directly below the metaconid
	21	Point on the CEJ directly below the entoconid
	22	Point on the CEJ directly below the below where the preentocristid and postmetacristid meet
	23	Point on the CEJ directly below the metaconid
Maxillary M^2	1	Paracone apex
	2	Protocone apex
	3	Hypocone apex
	4	Metacone apex
	5	Mesial-most point on occlusal surface
	6	Distal-most point on occlusal surface
	7	Lowest point on the crista obliqua – usually at the midline
	8	Lowest point on the entocrista
	9	Intersection of the postparacrista and premetacrista
	10	Lowest point in the trigon basin
	11	Lowest point in the talon basin
	12	Point of maximum curvature directly below the protocone
	13	Point of maximum curvature directly below point 8
	14	Point of maximum curvature directly below the hypocone
	15	Point on the CEJ directly below the protocone
	16	Point on the CEJ directly below point 13
	17	Point on the CEJ directly below the hypocone
	18	Point of maximum curvature directly below the paracone
	19	Point of maximum curvature directly below the intersection of the postparacrista and premetacrista
	20	Point of maximum curvature directly below the metacone
	21	Point on the CEJ directly below the paracone
	22	Point on the CEJ directly below the below the intersection of the postparacrista and premetacrista
	23	Point on the CEJ directly below the metacone

variable, since this allowed us to adjust for allometry using the same biomechanically relevant size variable across all datasets. For all of the PLS analyses where the diet matrix was included, we used PLS code adjusted from the "geomorph" package to accommodate a single non-morphological dataset. Statistical significance of the PLS correlations was assessed using a permutation test (9,999 iterations) where the objects in one data matrix were permuted relative to the other data matrix.

Covariance among the dental and cranial datasets was assessed using PLS analysis, also using the phylogeny and size (i.e., mandible length) adjusted regression residuals. As with the PLS analyses involving the diet matrix, we present the PLS correlation (Klingenberg, 2009) between the first singular warp axes for each dataset and the RV coefficient describing the overall relationship between the two blocks of data. We visualized the relationship between each of the datasets being examined by plotting the PLS scores, and we examined the corresponding wireframe diagrams for the morphological datasets. The significance of these PLS analyses was assessed using a permutation test with 9,999 iterations. For all analyses our critical alpha was set at 0.05, and we corrected for Type I error by employing a sequential Bonferroni adjustment (Rice, 1989).

RESULTS

Phylogeny and Size

A statistically significant phylogenetic signal was found for all datasets except the mandibular condyle (Fig. 4). Furthermore, the multivariate regression

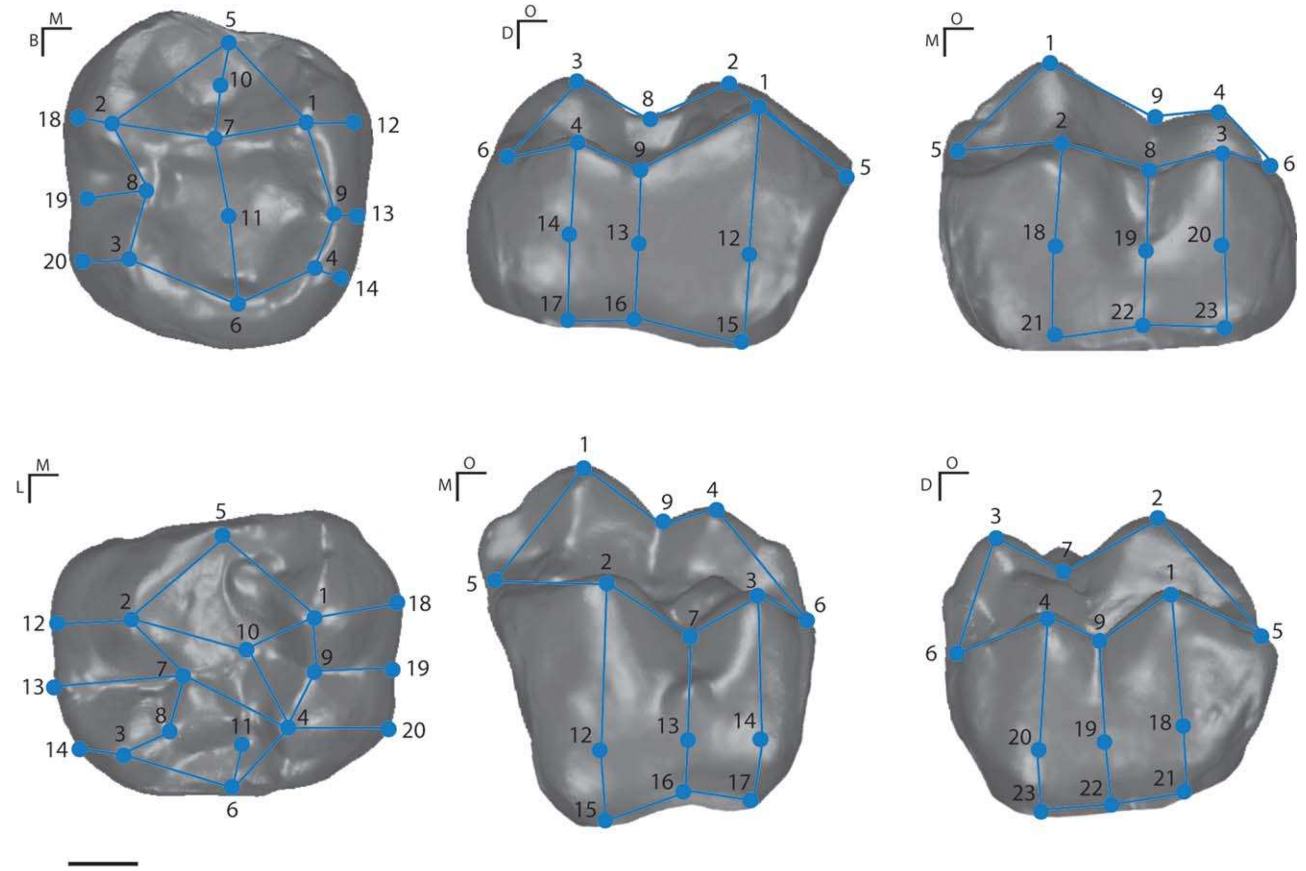

Fig. 3. Lower M_2 (top) and upper M^2 (bottom) of *Cebus capucinus* in (left to right) occlusal, lingual, and buccal views showing landmarks and wireframes employed in this study. Directional indictors are shown for each tooth: distal, D; mesial, M; occlusal, O; lingual, L; buccal, B. Landmark numbers correspond to those listed in Table 2. Scale bar is 1 mm.

analyses (Table 4) indicate that there is allometric variation in the data, with both the glenoid and overall cranial datasets significantly related to both log centroid size (of their respective configurations) and the natural log of mandibular length. These relationships disappeared, however, when the PGLS regression analyses were performed. These results therefore suggest that size tracks phylogeny in this sample, and that both phylogenetic and allometric patterning in the dataset should be taken into account in all subsequent analyses.

Covariance With Diet

The diet tree (Fig. 5) mirrors the phylogenetic tree in some general branching patterns. In particular, the pitheciines have a dietary make-up distinct from other platyrrhines and are the basal lineage in both the diet tree and in the phylogenetic tree. Both species of *Alouatta* are also dietarily distinct and this genus is a sister taxon to *Saimiri* and the frugivores. Amongst the cebids and atelids, there is more dietary diversity than among the pitheciines; consequently, branching patterns on the dietary tree do not mirror phylogeny to as great an extent as in pitheciines.

The PLS analyses where the diet matrix was included revealed a significant relationship between diet and the upper molar, lower molar, and cranial datasets (Table 5). However, none of these relationships were significant after the sequential Bonferroni correction. In all three of these analyses, the PLS plots (Fig. 6) reveal that the pitheciines all cluster relatively closely together to the exclusion of the other taxa, both in morphology (*x* axis) and in diet (*y* axis). There does not appear to be a strong differentiation in either diet or morphology for the remaining taxa.

Covariance Among Morphological Datasets

Results of the PLS analyses using the PGLS regression residuals of shape regressed on the natural log of mandible length indicate significant relationships between upper and lower molar form and cranial, glenoid, and mandibular form (Table 6). Because the bulk of research on dental form and its relationship to diet has examined the lower molars, we discuss only the results for the lower molar here. The overall patterns of shape variation for the upper molar were very similar to those observed for the lower molar (see Supporting Information).

Cranium and glenoid fossa versus lower molar. There is a significant relationship ($P = 0.01$) between cranial and lower molar shape, as demonstrated by the PLS plot of these two datasets (Fig. 7). At the

TABLE 3. Diet matrix

Species	Fruit	Animal	Leaves	Seeds	Flowers	Other	References
Alouatta palliata	37.17[a]	0.0	50.2	0.0	10.9	0.0	Milton, 1980; Chapman, 1987; Estrada et al. 1999
Alouatta seniculus	33.9[a]	0.0	54.5	0.0	9.0	0.1	Gaulin and Gaulin, 1982; Julliot and Sabatier, 1993
Ateles geoffroyi	75.6[a]	0.4	16.4	0.0	6.0	0.9	Chapman, 1987; Campbell, 2000; Russo et al., 2005; Gonzalez-Zamora et al., 2009
Lagothrix lagotricha	75.9	3.6	10.3	7.2	2.4	0.1	Soini, 1986; Peres, 1994; Defler and Defler, 1996; Di Fiore, 2004
Aotus trivirgatus	72.5	15.0	4.0	0.0	15.0	0.0	Wright, 1989
Cebus capucinus	81.2	16.9	1.3	0.0	0.2	0.0	Chapman, 1987
Saimiri sciureus	63.5	33.0	0.0	0.0	2.1	0.0	Lima and Ferrari, 2003; Pinheiro et al., 2013
Cacajao melanocephalus	10.5	2.4	10.8	68.3	7.2	0.8	Barnett, 2010
Chiropotes satanas	26.4	0.2	0.2	69.1	2.8	0.5	Ayers, 1989; Kinzey and Norconk, 1993; van Roosmalen et al., 1998
Pithecia pithecia	26.5	2.7	6.4	61.9	2.0	0.0	Kinzey and Norconk, 1993; Norconk and Conklin-Brittain, 2004

[a] % seeds not reported separately for these taxa.

negative end of both axes, the pitheciines tend to cluster together along with *C. capucinus*, and represent a morphotype with a relatively flexed cranial base, an anteroposterior short cranium with a small face relative to the neurocranium, and laterally flaring zygomatics with a laterally situated glenoid fossa relative to the tooth row. The glenoid fossa in these taxa is also relatively wide and anteroposteriorly (AP) short. In the dentition, these taxa exhibit relatively quadrate tooth forms with low cusps and short shearing crests.

The two *Alouatta* species fall at the extreme positive ends of both of these axes, and are closest in morphospace to *Aotus* and *Saimiri*. These taxa, particularly *Alouatta*, are represented by large faces relative to their neurocrania; for *Aotus* this likely reflects increased orbit size. These taxa also exhibit mediolaterally (ML) long crania, with tooth rows shifted laterally to lie closer to the AP elongated glenoid fossa. In the dentition, these taxa exhibit relatively mesio-distally long molars, with taller cusps. The combination of tall cusps that are more widely spaced allows for longer shearing crests.

Glenoid fossa versus lower molar. There is also a strong and significant relationship ($P = 0.002$) between glenoid fossa shape and the morphology of the lower molar (Fig. 8). As with the analysis of both the cranium and glenoid, the pitheciines fall at the negative end of both the glenoid and lower molar axes, and the two species of *Alouatta* fall at the extreme positive ends of these axes. Dental form along these axes is identical to that described above: pitheciines (particularly *Chiropotes* and *Cacajao*) have teeth that are more quadrate in form, with low cusps and short shearing crests, whereas *Alouatta* and *Saimiri* exhibit lower molars that are mesio-distally elongated and have high cusps with long shearing crests. In the glenoid fossa, the pitheciines exhibit ML wider joints with smaller postglenoid processes, while *Alouatta* (and *Saimiri*) have glenoid fossae that are anteroposterior long, ML narrow, and have relatively large postglenoid processes. There appears to be very little difference in the size or projection of the entoglenoid process among taxa, however.

Mandible and condyle versus lower molar. Mandibular form covaries significantly ($P = 0.001$) with lower molar form as well (Fig. 9). Again, we see a strong differentiation between *Alouattta* and the pitheciines. As with the analysis of cranial form, *Cebus* appears much more similar to the pitheciines (particularly *Chiropotes* and *Cacajao)* in mandibular shape. Variation in lower molar form is the same as discussed above. Mandibular form primarily varies in relation to the height of the condyle above the occlusal plane, and the relative size and curvature of the mandibular condyle. The pitheciines exhibit TMJs that are relatively closer to the occlusal plane, and they also have more ML curved condyles, while *Alouatta* has TMJs situated very high above the occlusal plane, and condyles that are relatively small and ML flat.

Mandibular condyle versus lower molar. The relationship between mandibular condyle and lower molar shape was not found to be statistically significant ($P = 0.3$).

DISCUSSION

The results obtained here generally support our initial hypotheses regarding covariation between dental and TMJ form. It is not surprising that molar and TMJ morphology covary, but the extent of the covariation across taxa differing in body-size and diet (e.g., *Alouatta* and *Saimiri*) indicates strong selection for (1) maintaining precise occlusion in forms that emphasize shearing as their major form of dental preparation of food items, and (2) increasing the amount of lateral deviation of the mandible in those taxa that habitually consume hard objects and have a substantial crushing component to their mastication (e.g., the pitheciines). While Hylander (1979) hypothesized this outcome, this article is the first to directly examine covariation between these parts of

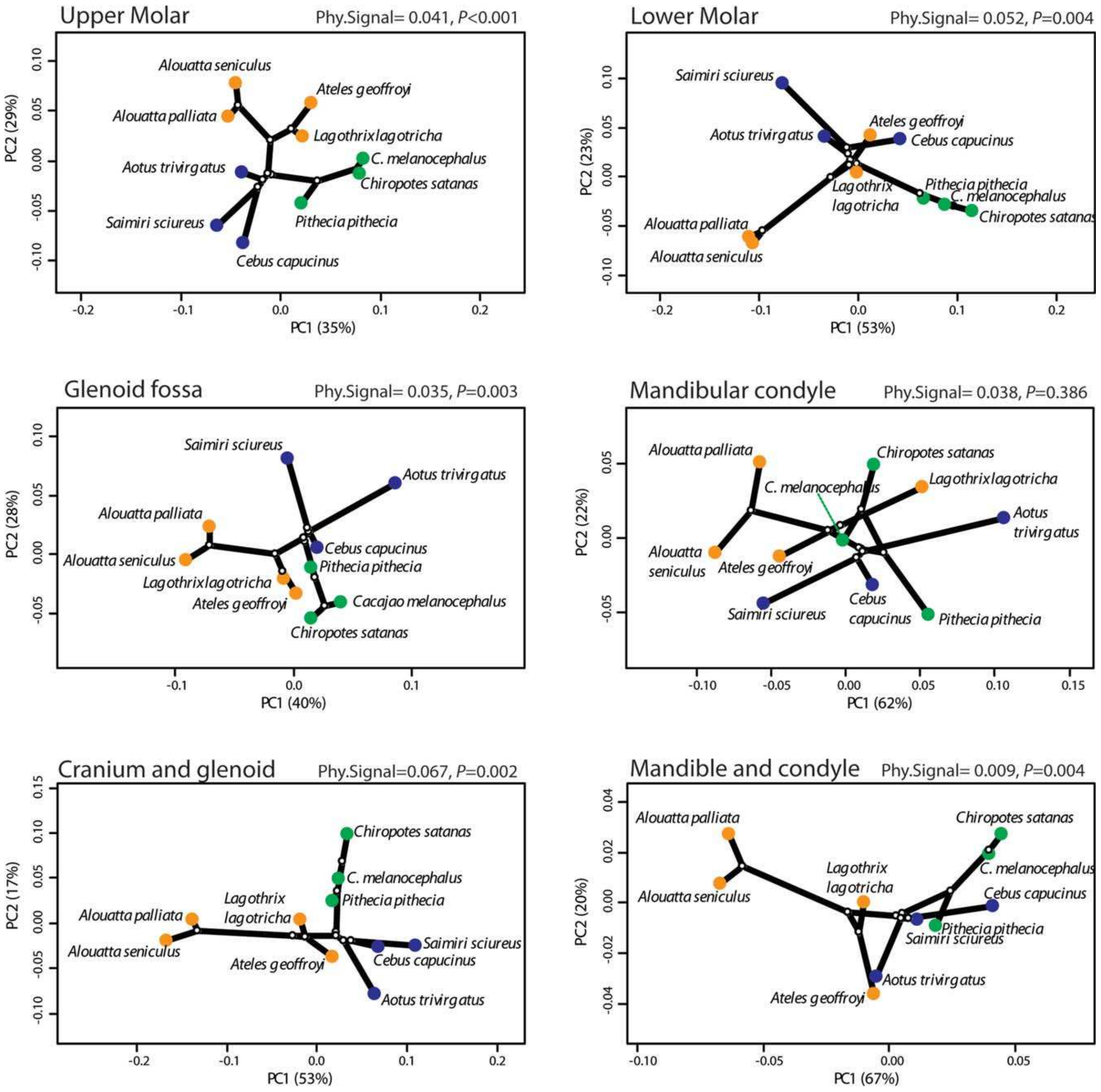

Fig. 4. Principal component plots of the first two PC axes for each of the six datasets. Plots include overlays of the consensus phylogenetic tree to illustrate the relationship between shape and phylogeny. Phy.Signal = the sum of squared changes in shape along the branches of the consensus phylogeny; *P* values represent the significance of the phylogenetic signal for each dataset. All relationships are significant after sequential Bonferroni correction, except for the mandibular condyle dataset.

the masticatory apparatus. Further analyses validating these proposed kinematic patterns will allow us to build upon this work and to better understand the precise movements of the condyles and teeth during mastication.

Covariance Between Dental and Cranial Form

Saimiri and *Alouatta* both have highly crowned/crested teeth and morphologies that likely act to guide mediolateral movements of the condyle, which we suggest allows the shearing crests to come into precise occlusion. These morphologies include mediolaterally narrow glenoids, with slightly more anteriorly inclined articular eminences, and large postglenoid processes. These latter two features were not predicted to vary significantly in relation to lateral deviation, while entoglenoid process size, which we did predict to vary, was not substantially different among the taxa sampled here. *Saimiri* and *Alouatta* also share many aspects of overall

TABLE 4. Regression results for shape regressed on the natural log of centroid size (LnCS) and the natural log of mandible length (LnMandLg)

	Phylogeny not incorporated into regression				PGLS regressions			
	Shape ~ LnCS		Shape ~ LnMandLg		Shape ~ LnCS		Shape ~ LnMandLg	
	%variance	*P* value	%variance	*P* value	%variance	*P* value	%variance	*P* value
Upper molars	19.84	0.064	18.79	0.085	15.10	0.720	18.31	0.387
Lower molars	19.15	0.128	14.50	0.242	17.71	0.428	13.89	0.530
Glenoid fossa	**31.61**	**0.001**	**28.46**	**0.006**	25.63	0.120	22.26	0.280
Mandibular condyle	18.16	0.165	16.27	0.209	13.21	0.456	9.90	0.689
Cranium and glenoid	**33.43**	**0.014**	**38.73**	**0.005**	26.57	0.164	32.77	0.121
Mandible and condyle	26.69	0.070	22.51	0.107	14.54	0.542	11.14	0.624

Values represent the percentage variance explained by the regression (%variance) and the corresponding *P* value. Relationships significant at $P < 0.05$ are shown in bold, relationships significant after the sequential Bonferroni correction are highlighted in gray.

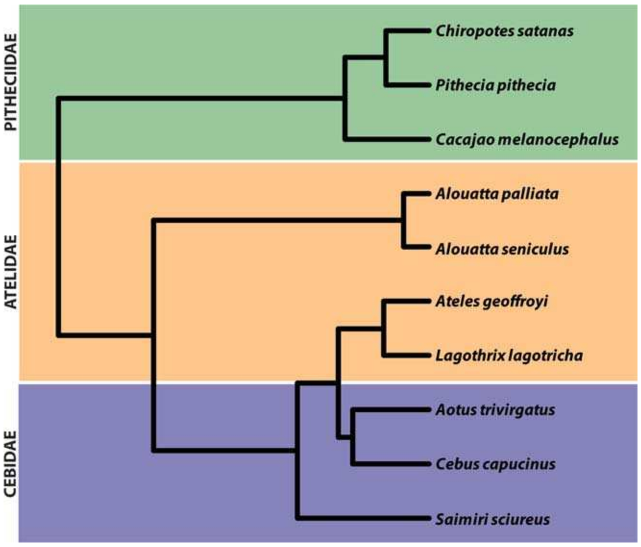

Fig. 5. Unweighted pair group method average (UPGMA) tree describing dietary similarities in taxa based on the dietary matrix (as provided in Table 3).

TABLE 5. Results of the two-block partial least squares analyses of the diet matrix vs. each of the morphological datasets

Diet vs.	PLS	*P* value	RV	*P* value
Upper molars	0.909	0.015	0.620	0.008
Lower molars	0.882	0.017	0.650	0.012
Glenoid fossa	0.834	0.103	0.450	0.065
Cranium and glenoid	0.914	0.017	0.559	0.013
Mandibular condyle	0.542	0.691	0.128	0.809
Mandible and condyle	0.806	0.047	0.499	0.038

Partial least squares correlations (PLS) and RV coefficients (RV) are both provided along with their corresponding *P* values. Bolded values are significant at $P < 0.05$ (no values were significant after sequential Bonferroni correction). All datasets employed the size (log mandible length) and phylogeny adjusted regression residuals.

cranial form, such as large faces relative to the neurocranium and ML narrow, AP long crania. While many of these similarities in dental and glenoid morphology were expected for *Alouatta* and *Saimiri, Aotus* also showed similar morphologies of the teeth, TMJ, and overall cranium (i.e., somewhat longer shearing crests and higher occlusal relief in combination with a more laterally shifted tooth row, a smaller flatter condyle, and a larger face). Relatively few dietary data exist for *Aotus*, but the few that do exist do not indicate that members of this genus consume a substantial quantity of insects or leaves. The results of this study suggest, however, that at least the dentition is under selective pressure to maintain a higher degree of shear than in other frugivorous taxa. However, it is also important to keep in mind that its very large orbits and relatively less flexed cranial base (Ross and Ravosa, 1993) may be driving some of the cranial similarities with *Alouatta* in particular. For example, in the PLS plot of the cranium/glenoid and lower molar analysis (see Fig. 7), *Aotus* falls within the range of *Alouatta* on the Y-axis, but when data are partitioned so that only glenoid fossa landmarks are included, *Aotus* exhibits a far more generalized morphology with mediolaterally wide glenoids and smaller postglenoid process. Thus, it seems likely that the large orbits and less flexed cranial base of *Aotus* are driving its overall cranial similarity to *Alouatta*.

In contrast to "shearing" forms, the pitheciines appear to have glenoid morphologies that facilitate lateral deviation during chewing, including ML wide glenoids and less inclined articular eminences. *Chiropotes* and *Cacajao* are more extreme in this morphology than *Pithecia*, a result consistent with both the dietary data indicating that *Pithecia* may be somewhat less specialized for consuming hard seeds (Ledogar et al., 2013), and the phylogenetic tree showing *Pithecia*'s position as the basal member of this clade (Perelman et al., 2011). Additionally, all pitheciine species possess dentition with low cusp relief, an adaption to crushing hard food items.

While not as extreme in its adaptations to consuming hard objects as the pitheciines, *Cebus capucinus* often fell with the pitheciines in our analyses. The diet of this taxon, however, is not nearly as hard object focused as that of *Cebus apella* (e.g., Terborgh, 1983), which also has unique dental adaptations including very thick enamel (Martin et al., 2003). While *Cebus capucinus*

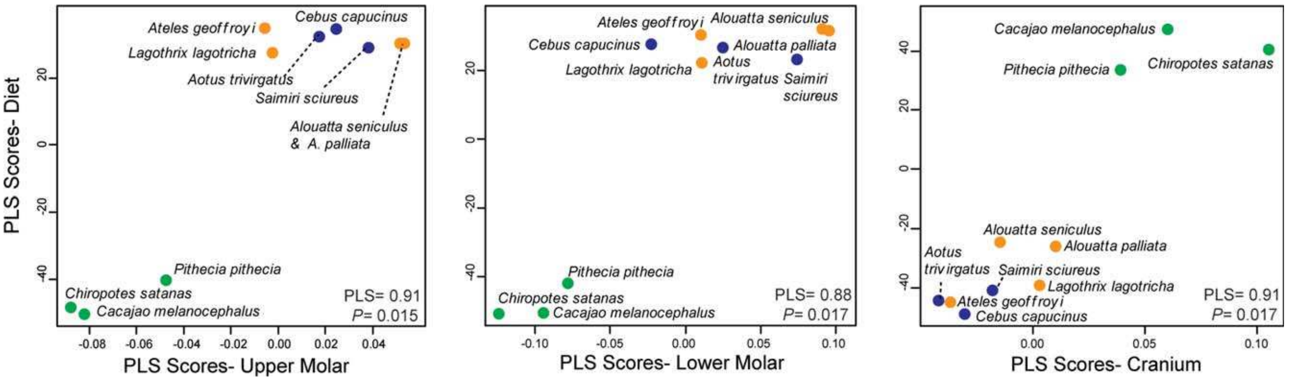

Fig. 6. Two-block partial least squares (PLS) plots for the analyses comparing the diet matrix to the morphological matrices. Only plots for the marginally significant ($P < 0.05$) relationships are shown here. Corresponding RV coefficients are presented in Table 5.

TABLE 6. Results of the two-block partial least squares (PLS) analyses of the dental vs. cranial and mandibular datasets

	Upper molars				Lower molars			
	PLS	*P* value	RV	*P* value	PLS	*P* value	RV	*P* value
Glenoid fossa only	0.962	0.001	0.784	0.001	0.954	0.002	0.789	0.001
Mandibular condyle only	0.747	0.536	0.376	0.317	0.69	0.3	0.358	0.178
Cranium and glenoid	0.938	0.013	0.753	0.001	0.917	0.01	0.712	0.002
Mandible and condyle	0.961	0.001	0.706	0.001	0.952	0.001	0.860	0.0002

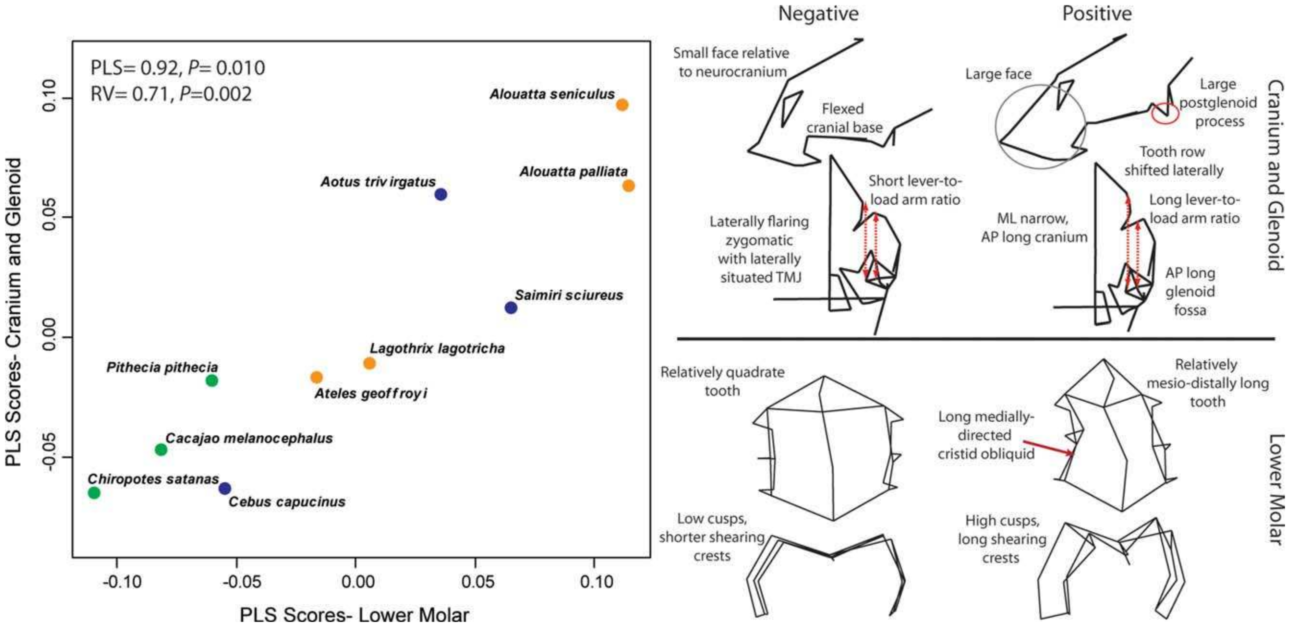

Fig. 7. Bivariate plot of the partial least squares (PLS) scores for the lower M_2 (x axis) versus the cranium and glenoid (y axis). The PLS correlation (PLS) and corresponding wireframes on the right illustrate shape variation along each of these axes. The RV coefficient describes the overall relationship between the two blocks of data. Refer to Figs. 2 and 3 for more information on the wireframes.

does not specialize in hard objects per se, it clearly has overlapping morphology with taxa that do, begging the question of whether the ancestral condition for this genus might be hard object consumption. While our study does not include *Cebus apella* among those primates sampled, a comparison of the *Cebus* species would be instructive for understanding dietary adaptation and evolution among the cebids.

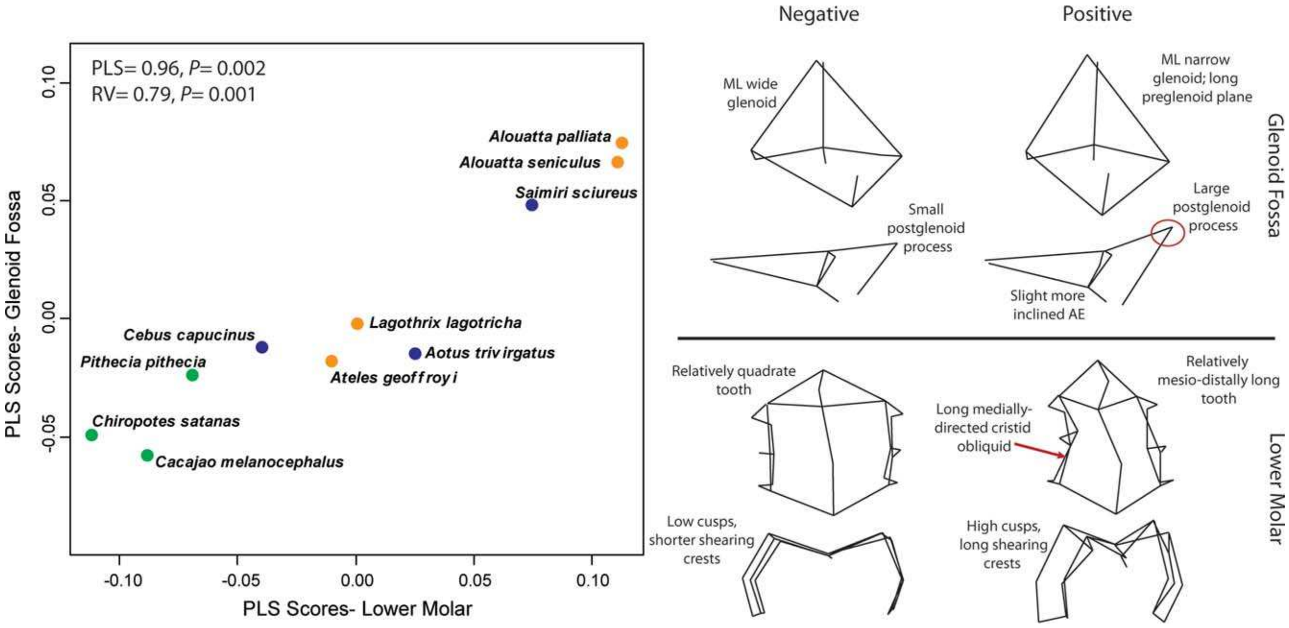

Fig. 8. Bivariate plot of the partial least squares (PLS) scores for the lower M_2 (*x* axis) versus the glenoid fossa (*y* axis). The PLS correlation (PLS) and corresponding Wireframes on the right illustrate shape variation along each of these axes. The RV coefficient describes the overall relationship between the two blocks of data. Refer to Figs. 2 and 3 for more information on the wireframes.

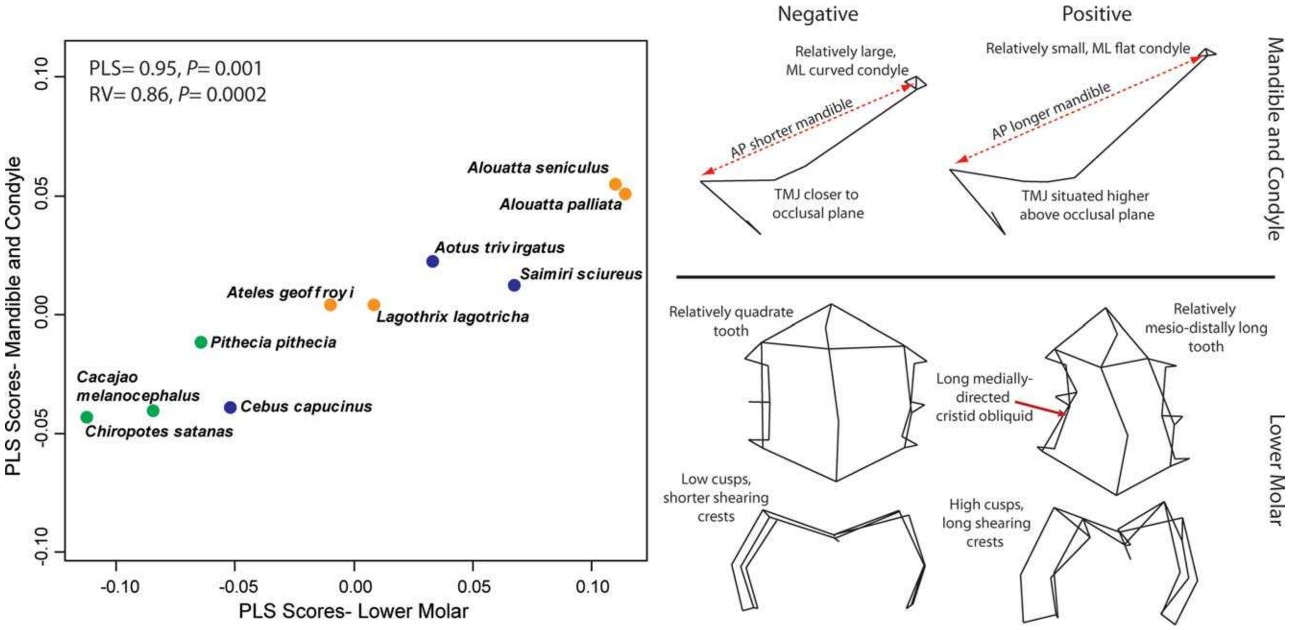

Fig. 9. Bivariate plot of the partial least squares (PLS) scores for the lower M_2 (*x* axis) versus the mandible and condyle (*y* axis). The PLS correlation (PLS) and corresponding Wireframes on the right illustrate shape variation along each of these axes. The RV coefficient describes the overall relationship between the two blocks of data. Refer to Figs. 2 and 3 for more information on the wireframes.

The frugivorous primates, *Ateles* and *Lagothrix*, fell in the middle of our distributions and show a generalized intermediate morphology. Both of these taxa are soft fruit specialists with no substantial consumption of either hard objects or foods requiring extensive oral preparation. Indeed, *Ateles* and *Lagothrix* are important seed dispersers in neotropical forests, and many of the fruits consumed contain large pits that are swallowed whole (Link and Di Fiore, 2006; Di Fiore et al., 2008). Interestingly, *Ateles* exhibits relatively short chew cycle durations for its jaw length (Ross et al., 2009), and members of this genus have smaller than predicted physiological cross-sectional areas for the temporalis and superficial masseter (Taylor et al., 2012). Together these data suggest that *Ateles* (and presumably *Lagothrix*, although few data are available for this genus) have relatively generalized masticatory morphologies which are not optimized for generating large bite forces, and that they do not spend a large percentage of their time actively masticating food items.

Although we didn't test specific hypotheses for how dental and overall skull form would covary in our sample, our data do allow us to make several unique observations about variation in masticatory form among taxa in our sample. In particular, the analysis of overall cranial form reveals a gradation in the position of the tooth row relative to the TMJ, and in the position of the bite point relative to the most anterior attachment of the superficial masseter. In pitheciines, we observed more laterally flaring zygomatics, TMJs positioned more laterally relative to the toothrow, and a more anteriorly positioned superficial masseter attachment relative to the molars. Such a configuration would be very advantageous for generating high bite forces in these taxa. Widely flaring zygomatics would allow these taxa to exert more laterally directed muscle force from the superficial masseter and medial pterygoids; a TMJ positioned farther away laterally from the tooth row would increase the area of Greaves' triangle of support (Greaves, 1978), which would decrease the likelihood of TMJ distraction when biting on very hard objects far back on the tooth row (Spencer, 1995, 1999); and a more anteriorly positioned attachment of the masseter decreases the lever-to-load arm ratio which would allow more muscle force to be converted into bite force. Conversely, *Alouatta* has relatively less flaring zygomatics, a TMJ situated ML closer to the toothrow, and a more posteriorly positioned superficial masseter attachment relative to the molars; these bite forces is not as important in this taxon.

Although condylar form when examined in isolation from the rest of the mandible did not significantly covary with dental form in our sample, condylar form when examined as part of the mandible did significantly covary with the dentition. This result suggests that perhaps there were too few landmarks ($n = 5$) describing condylar form, and that it is only by coupling these landmarks with other landmarks describing the overall position of the condyle that the results are significant. This analysis did reveal several interesting results in terms of condylar form. As with the cranium, the PLS analysis of the mandible/condyle versus the lower molars revealed that *Alouatta*, and to a lesser extent *Aotus* and *Saimiri*, have relatively smaller, ML flatter condyles that are situated relatively farther above the occlusal plane. Conversely, the pitheciines and *Cebus* tended to have relatively larger, ML curved condyles that were situated closer to the occlusal plane. While *Alouatta* does indeed have condyles situated well above the occlusal plane, it is most likely that this morphology is less related to dietary variation than it is to the need of members of this genus to accommodate their enlarged hyoid apparatus, though it will potentially have a strong mechanical effect and thus be indirectly linked to masticatory function and diet. The observed variation in relative condylar size is particularly striking, and bears further study. Univariate analyses of condylar area in platyrrhines have not revealed a systematic pattern of condylar size variation among closely related taxa (Terhune, 2011a), but the relative size differences hinted at here suggest that condylar size is relatively larger in pitheciines. This is consistent with the potential for members of this clade to dissipate relatively larger joint reaction forces and reduce joint stress while masticating very hard food items.

Craniodental Morphology and Diet

The dietary data used in this article were drawn from the literature and as a consequence collection methods across studies were not consistent. There were several ways in which data differed: (1) dietary categories (2) study length. For the former, the main difference involved whether or not seeds were reported as a separate category from fruit—in *Alouatta* and *Ateles* they were not, which, given that these taxa do not for the most part chew or digest seeds, may matter very little. The length of time that a group of primates is observed can have a large effect on the dietary data collected, however. Over the course of the year, there is substantial variation in the types of foods available and if a primate group is only observed during a small portion of the year, dietary data may not reflect the annual diet.

Most importantly, these data are only rough proxies for the material properties of food items. Food material properties, such as fracture resistance and toughness, would be the most ideal values against which to assess dental and cranial morphology, as these properties will be most proximately related to craniodental variation. Unfortunately, relatively few data are available on food items consumed by the platyrrhines (e.g., Norconk et al., 2009), making such an analysis impossible until additional food material property data are collected. Nevertheless, our analyses indicate covariation between diet and the morphology of the masticatory complex (Fig. 6). The pitheciines are most dietarily distinct as they specialize in a food item (i.e., seeds) not consumed in any substantial quantity by the other taxa included in this study. They also have very distinctive molar and cranial morphologies, which sets them apart in morphospace. This result is consistent with the suggestion of a deep phylogenetic divergence for this clade, estimated at around 20 million years (Perelman et al., 2011), which, combined with the presence in the fossil record of primates with pitheciine-like dental morphology in the Early and Middle Miocene (Fleagle, 1990; Kay et al., 1998) indicates that seed predation is an ancient dietary niche for the pitheciine clade. We saw no corresponding strong differentiation between the atelids and cebids, however, all of which tended to cluster together in the dietary analyses. This is perhaps reflective of both their more recent phylogenetic divergence and relationship as sister groups (Perelman et al., 2011) as well as their more similar dietary regimes, as shown in Fig. 5.

Accounting for Size and Phylogeny

One interesting result of this analysis was the clustering of the smallest bodied primates, *Aotus* and *Saimiri*, with one of the largest bodied primates, *Alouatta*. While this result is consistent with what we know about the diets of these species, this result is not necessarily intuitive given the large differences in body size, and thus potential allometric differences in craniodental form, among these taxa. Furthermore, as demonstrated here, all of these datasets (except the condyle) show a significant phylogenetic signal. Thus, it was necessary to also control for covariance due to shared phylogenetic history.

By performing a multivariate PGLS regression of the shape coordinates onto the natural log of mandibular length and using these regression residuals in all further analyses, we were successfully able to correct for phylogenetic covariance, and we were able to examine meaningful differences in craniodental form relative to a biomechanically significant scaling variable. Preliminary analyses that did not account for this phylogenetic and size variation showed strong clustering of taxa on the basis of these two variables alone, and any dietary signal present in the data was swamped. Thus, although this analysis is limited in scope due to the relatively small sample sizes employed, we hope that this study can serve as a test case for further analyses seeking to assess functional signals in phylogenetically diverse samples that span a range of body sizes.

CONCLUSIONS

This study evaluated covariance between dental and cranial morphology in platyrrhine primates by linking these two datasets, which are often examined in isolation, in order to provide a more integrative understanding of diet-related morphology in this clade. While the finding that cranial/TMJ and dental shape covary in platyrrhines is not a surprising result, it is one that has not been previously demonstrated. Our results point to several important conclusions:

1. Primates exploiting food items requiring substantial dental processing (e.g., leaves or insects) have a high degree of dental shear coupled with cranial morphologies aimed at maintaining precise occlusion when vertical movement of the mandible during the powerstroke is emphasized.
2. Primates specializing in hard foods (e.g., seeds) have relatively shorter shearing crests and lower molar relief combined with a cranial morphology adapted to facilitate lateral deviation of the mandible during mastication.
3. Overall patterns of covariance between cranial and dental form do not fall along a gradient of dietary resistance, as has been demonstrated in platyrrhine primates previously (e.g., Norconk et al., 2009). Instead, this analysis separates taxa that utilize tough foods (e.g., *Alouatta*) and hard foods (e.g., *Chiropotes*), and more generalized (i.e., frugivorous) taxa are intermediate in form, though significantly more data on the material properties of foods need to be collected to fully evaluate the relationships between these variables.

With these findings in hand, we can begin to explore the ways in which morphological covariation correlates with diet, phylogeny, body size or other variables pertinent to an organism's ecological adaptations across a broader range of taxa. Further analyses will seek to examine whether similar patterns of shape covariation are found in taxonomic groups other than the small platyrrhine sample examined here, or whether there may be different morphological solutions for solving similar adaptive problems. While this study focuses on molar morphology, other tooth positions certainly affect mandibular movement during dental processing as well. Furthermore, these preliminary data linking cranial and dental form in platyrrhines will provide a set of testable hypotheses for future kinematic analyses designed to evaluate the precise movements of the condyles and teeth during mastication. It is also important to note here that although we hypothesize the bony and dental morphology play important roles in guiding the teeth into occlusion, soft-tissue structures and muscle activation patterns are likely also critical; future studies may therefore seek to marry these three diverse sources of data to better evaluate kinematic patterns in the masticatory apparatus.

ACKNOWLEDGEMENTS

The authors thank Eileen Westwig (AMNH) and Linda Gordon (NMNH) who facilitated access to primate specimens. For training in phylogenetic comparative methods, thanks go to Charlie Nunn and the AnthroTree Workshop. This manuscript was improved by comments from Christine Wall and Chris Robinson. This is NYCEP Morphometric Group manuscript number 87.

LITERATURE CITED

Adams DC, Otárola-Castillo E. 2013. Geomorph: An R package for the collection and analysis of geometric morphometric shape data. Methods Ecol Evol 4:393–399.

Anapol F, Lee S. 1994. Morphological adaptation to diet in platyrrhine primates. Am J Phys Anthropol 94:239–261.

Anderson K, Throckmorton GS, Buschang PH, Hayasaki H. 2002. The effects of bolus hardness on masticatory kinematics. J Oral Rehabil 29:689–696.

Arnold CLJ, Matthews L, Nunn CL. 2010. The 10kTrees website: a new online resource for primate phylogeny. Evol Anth 19:114–118.

Ayers JM. 1989. Comparative feeding ecology of the uakari and bearded saki, *Cacajao* and *Chiropotes*. J Hum Evol 18:697–716.

Barnett AA. 2010. Diet, habitat use and conservation ecology of the Golden-Backed Uacari, *Cacajao melanocephalus ouakary*, in Jau National Park, Amazonian Brazil. PhD Dissertation, Roehampton University.

Bookstein FL, Gunz P, MItteroecker P, Prossinger H, Schaefer K, Seidler H. 2003. Cranial integration in *Homo*: singular warps analysis of the midsagittal plane in ontogeny and evolution. J Hum Evol 44:167–187.

Bouvier M. 1986a. A biomechanical analysis of mandibular scaling in Old World monkeys. Am J Phys Anthropol 69:473–482.

Bouvier M. 1986b. Biomechanical scaling of mandibular dimensions in New World monkeys. Int J Prim 7:551–567.

Bouvier M, Hylander WL. 1984. The effect of dietary consistency on gross and histologic morphology in the craniofacial region of young rats. Am J Ant 170:117–126.

Boyer DM. 2008. Relief index of second mandibular molars is a correlate of diet among prosimian primates and other euarchontan mammals. J Hum Evol 55:1118–1137.

Byrd KE, Milberg DJ, Luschei ES. 1978. Human and macaque mastication: a quantitative study. J Dent Res 57:834–843.

Campbell CJ. 2000. The reproductive biology of black handed spider monkeys (*Ateles geoffroyi*): integrating behavior and endocrinology. PhD Dissertation, University of California, Berkeley.

Chapman C. 1987. Flexibility in the diets of three species of Costa Rican primates. Folia Primatol 49:90–105.

Constantino PJ. 2007. Primate masticatory adaptations to fracture resistant foods. PhD Dissertation, George Washington University.

Cooke SB. 2011. Paleodiet of extinct platyrrhines with emphasis on the Caribbean forms: three-dimensional geometric morphometrics of mandibular second molars. Anat Rec 294:2073–2091.

Daegling DJ. 1989. Biomechanics of cross-sectional size and shape in the hominoid mandibular corpus. Am J Phys Anthropol 80:91–106.

Daegling DJ. 2007. Relationship of bone utilization and biomechanical competence in hominoid mandibles. Arch Oral Biol 52:51–63.

Defler TR, Defler SB. 1996. Diet of a group of *Lagothrix lagothricha lagothricha* in Southeastern Colombia. Int J Primatol 17:161–190.

Di Fiore A. 2004. Diet and feeding ecology of woolly monkeys in a western Amazonian rainforest. Int J Primatol 25:767–801.

Di Fiore A, Link A, and Dew JL, 2008. Diets of wild spider monkeys. In: Campbell CJ, editor. Behavior, ecology and evolution of the genus *Ateles*. Cambridge: Cambridge University Press. p 81–137.

DuBrul EL. 1977. Early hominid feeding mechanisms. Am J Phys Anthropol 47:305–320.

Estrada A, Juan-Solano S, Ortiz Martinez T, Coates-Estrada R. 1999. Feeding and general activity patterns of a howler monkey (*Alouatta palliata*) troop living in a forest fragment at Los Tuxtlas, Mexico. Am J Primatol 48:167–183.

Evans AR, Wilson GP, Fortelius M, Jernvall J. 2007. High-level similarity of dentitions of carnivorans and rodents. Nature 445:78–81.

Fleagle JG. 1990. New fossil platyrrhines from the Pinturas Formation, southern Argentina. J Hum Evol 19:61–83.

Ford SM, Davis LC. 1992. Systematics and body size: implications for feeding adaptations in New World monkeys. Am J Phys Anthropol 88:415–468.

Freeman PW. 1988. Frugivorous and animalivorous bats (Microchiroptera): dental and cranial adaptations. Biol J Linn Soc 33:249–272.

Garland T, Jr, Ives AR. 2000. Using the past to predict the present: confidence intervals for regression equations in phylogenetic comparative methods. Am Nat 155:346–364.

Gaulin SJC, Gaulin CK. 1982. Behavioral ecology of *Alouatta seniculus* in Andean Cloud Forest. Int J Primatol 3:1–32.

Gonzalez-Zamora A, Arroyo-Rodriguez V, Chaves OM, Sanchez-Lopez S, Stoner KE, Riba-Hernandez P. 2009. Diet of spider monkeys (*Ateles geoffroyi*) in Mesoamerica: current knowledge and future directions. Am J Primatol 71:8–20.

Goodall C. 1991. Procrustes methods in the statistical analysis of shape. J R Stat Soc B 53:285–339.

Grafen A. 1989. The phylogenetic regression. Phil Trans R Soc B 326:119–157.

Greaves WS. 1974. Functional implications of mammalian jaw joint position. Forma Funct 7:363–376.

Greaves WS. 1978. The jaw lever system in ungulates: a new model. J Zool Lond 184:271–285.

Greaves WS. 1980. The mammalian jaw mechanism—the high glenoid cavity. Am Nat 116:432–440.

Gregory WK. 1922. The origin and evolution of the human dentition. Baltimore: Williams and Wilkins.

Herring SW, Herring SE. 1974. The superficial masseter and gape in mammals. Am Nat 108:561–576.

Hiiemae KM. 1978. Mammalian mastication: a review of the activity of the jaw muscles and the movements they produce in chewing. In: Butler PM, Joysey KA, editors. Development, function and evolution of teeth. London: Academic Press. p 359–398.

Hiiemae KM, Crompton AW. 1985. Mastication, food transport and swallowing. In: Hildebrand ME, Bramble DM, Liem KF, editors. Functional vertebrate morphology. Cambridge: Harvard University Press. p 262–290.

Hylander WL. 1979. Functional significance of primate mandibular form. J Morphol 160:223–240.

Hylander WL. 1984. Stress and strain in the mandibular symphysis of primates: a test of competing hypotheses. Am J Phys Anthropol 64:1–46.

Hylander WL. 1985. Mandibular function and biomechanical stress and scaling. Am Zool 25:315–330.

Hylander WL. 1988. Implication of *in vivo* experiments for interpreting the functional significant of "robus" australopithecine jaws. In: Grine FE, editor. The evolutionary history of the "robust" australopithecines. New York: Aldine de Gruyter. P 55–83.

Hylander WL, Bays R. 1979. An *in vivo* strain-gauge analysis of the squamosal-dentary joint reaction force during mastication and incisal biting in *Macaca mulatta* and *Macaca fascicularis*. Arch Oral Biol 24:689–697.

Iriarte-Diaz J, Terhune CE, Taylor AB, Ross CF. 2013. Mandibular helical axis during feeding in non-human primates. Am J Phys Anthropol 150(S56):157.

Janson CH, Boinski S. 1992. Morphological and behavioral adaptations for foraging in generalist primates: the case of the cebines. Am J Phys Anthropol 88:483–498.

Julliot C, Sabatier D. 1993. Diet of the red howler monkey (*Alouatta seniculus*) in French Guiana. Int J Primatol 14:527–550.

Kay RF. 1975. The functional adaptations of primate molar teeth. Am J Phys Anthropol 43:195–216.

Kay RF. 1978. Molar structure and diet in extant Cercopithecidae. In: Butler PM, Joysey KA, editors. Development, function and evolution of teeth. London: Academic Press. p 309–333.

Kay RF. 1984. On the use of anatomical features to infer foraging behavior in extinct primates. In: Rodman PS, Cant JGH, editors. Adaptations for foraging in nonhuman primates: contributions to an organismal biology of prosimians, monkeys and apes. New York: Columbia University Press. p 21–53.

Kay RF, Covert HH. 1984. Anatomy and behaviour of extinct primates. In: Chivers DJ, Wood BA, Bilsborough A, editors. Food acquisition and processing in primates. New York: Plenum. p 467–508.

Kay RF, Hiiemae KM. 1974. Jaw movement and tooth use in recent and fossil primates. Am J Phys Anthropol 40:227–256.

Kay RF, Hylander W. 1978. The dental structure of mammalian folivores with special reference to primates and phalangeroidea (Marsupialia). In: Montgomary GG, editor. The biology of arboreal folivores. Washington DC: Smithsonian Institution Press. p 173–191.

Kay RF, Johnson D, Meldrum DJ. 1998. A new pitheciine primate from the middle Miocene of Argentina. Am J Primatol 45:317–336.

Kinzey WG, Norconk MA. 1993. Physical and chemical properties of fruit and seeds eaten by *Pithecia* and *Chiropotes* in Surinam and Venezuela. Int J Primatol 14:207–227.

Klingenberg CP. 2009. Morphometric integration and modularity in configurations of landmarks: tools for evaluating a priori hypotheses. Evol Dev 11:405–421.

Komiyama O, Asano T, Suzuki H, Kawara M, Wada M, Kobayashi K, Ohtake S. 2003. Mandibular condyle movement during mastication of foods. J Oral Rehabil 30:592–600.

Ledogar JA, Winchester JM, St. Clair EM, Boyer DM. 2013. Diet and dental topography in Pitheciine seed predators. Am J Phys Anthropol 150:107–121.

Lima EM, Ferrari SF. 2003. Diet of a free-ranging group of squirrel monkeys (*Saimiri sciureus*) in eastern Brazilian Amazonia. Folia Primatol 74:150–158.

Link A, Di Fiore A. 2006. Seed dispersal by spider monkeys and its importance in the maintenance of neotropical rain-forest diversity. J Trop Ecol 22:235–246.

M'Kirera F, Ungar P. 2003. Occlusal relief changes with molar wear in *Pan troglodytes troglodytes* and *Gorilla gorilla gorilla*. Am J Primatol 60:31–41.

Martin L, Olejniczak AJ, Maas MC. 2003. Enamel thickness and microstructure in pitheciin primates, with comments on dietary adaptations of the middle Miocene hominoid *Kenyapithecus*. J Hum Evol 45:351–367.

Maynard Smith J, Savage RJG. 1959. The mechanics of mammalian jaws. School Sci Rev 141:289–301.

Milton K. 1980. The foraging strategy of howler monkeys: a study in primate economics. New York: Columbia University Press.

Norconk MA, Conklin-Brittain NL. 2004. Variation on frugivoroy: the diet of Venezuelan white-faced sakis. Int J Primatol 25:1–26.

Norconk MA, Wright BW, Conklin-Brittain NL, Vinyard CJ. 2009. Mechanical and nutritional properties of food as factors in platyrrhine dietary adaptations. In: Garber PA, Estrada A, Bicca-Marques JC, Heymann EW, Strier KB, editors. South American primates: testing new theories in the study of primate behavior, ecology, and conservation. New York: Springer Science. p 279–319.

Osborne HF. 1907. The evolution of mammalian molar teeth. New York: Macmillan.

Owen R. 1845. Odontography or, a treatise on the comparative anatomy of the teeth: their physiological relations, mode of development, and microscopic structure, in the vertebrate animals. London: H. Baillière.

Perelman P, Johnson WE, Roos C, Seuánez HN, Horvath JE, Moreira MAM, Kessing B, Pontius J, Roelke M, Rumpler Y, Schneider MPC, Silva A, O'Brien SJ, Pecon-Slattery J. 2011. A molecular phylogeny of living primates. PLOS Genet 7:e1001342.

Peres CA. 1994. Diet and feeding ecology of gray woolly monkeys *(Lagothrix lagotricha cana)* in central amazonia: comparisons with other atelines. Int J Primatol 15:333–372.

Pinheiro T, Ferrari SF, Lopes MA. 2013. Activity budget, diet, and use of space by two groups of squirrel monkeys (*Saimiri sciureus*) in eastern Amazonia. Primates 54:301–308.

Ravosa MJ. 1990. Functional assessment of subfamily variation in maxillomandibular morphology among Old World monekys. Am J Phys Anthropol 82:199–212.

Ravosa MJ, Lopez EK, Menegaz RA, Stock SR, Stack MS, Hamrick MW. 2008. Adaptive plasticity in the mammalian masticatory complex: you are what, and how, you eat. In: Vinyard CJ, Ravosa MJ, Wall CE, editors. Primate craniofacial function and biology. New York: Springer. p 293–328.

Reed DA, Ross CF. 2010. The influence of food material properties on jaw kinematics in the primate, *Cebus*. Arch Oral Biol 55:946–962.

Rice WR. 1989. Analyzing tables of statistical tests. Evol 43:223–225.

Rohlf FJ. 2001. Comparative methods for the analysis of continuous variables: geometric interpretations. Evol 55:2143–2160.

Rohlf FJ, Corti M. 2000. Use of two-block partial least-squares to study covariation in shape. Syst Biol 49:740–753.

Rosenberger AL, Halenar L, Cooke SB. 2011. The making of platyrrhine semi-folivores: models of the evolution of folivory in primates. Anat Rec 294:2112–2130.

Rosenberger AL, Kinzey WG. 1976. Functional patterns of molar occlusion in platyrrhine primates. Am J Phys Anthropol 45:281–298.

Ross CF, Iriarte-Diaz J, Nunn CL. 2012. Innovative approaches to the relationship between diet and mandibular morphology in primates. Int J Primatol 33:632–660.

Ross CF, Ravosa MJ. 1993. Basicranial flexion, relative brain size, and facial kyphosis in nonhuman primates. Am J Phys Anthropol 91:305–324.

Ross CF, Reed DA, Washington RL, Eckhardt A, Anapol F, Shahnoor N. 2009. Scaling of chew cycle duration in primates. Am J Phys Anthropol 138:30–44.

Russo SE, Campbell CJ, Lawrence DJ, Stevenson PR, Suarez SA. 2005. A multi-forest comparison of dietary preferences and seed dispersal by *Ateles* spp. Int J Primatol 26:1017–1037.

Simpson GG. 1933. Paleobiology of Jurassic mammals. Paleobiol 5: 127–158.

Smith RJ, Petersen CE, Gipe DP. 1983. Size and shape of the mandibular condyle in primates. J Morphol 177:59–68.

Soini P. 1986. A synecological study of a primate community in the Pacaya-Samiria National Reserve, Peru. Primate Conserv 7:63–71.

Spencer MA. 1995. Masticatory system configuration and diet in anthropoid primates. PhD Dissertation, State University of New York at Stony Brook.

Spencer MA. 1999. Constraints on masticatory system evolution in anthropoid primates. Am J Phys Anthropol 108:483–506.

Stevens CE, Hume ID. 1995. Comparative physiology of the vertebrate digestive system. 2nd ed. New York: Cambridge University Press.

Taylor AB. 2002. Masticatory form and function in the African apes. Am J Phys Anthropol 117:133–156.

Taylor AB. 2005. A comparative analysis of temporomandibular joint morphology in the African apes. J Hum Evol 48:555–574.

Taylor AB. 2006. Feeding behavior, diet, and the functional consequences of jaw form in orangutans, with implications for the evolution of *Pongo*. J Hum Evol 50:377–393.

Taylor AB, Yuan T, Ross CF, Vinyard CJ. 2012. The scaling of jaw-muscle fiber architecture in anthropoid primates. Am J Phys Anthropol S56:269.

Terborgh J. 1983. Five new world primates. Princeton, NJ: Princeton University Press.

Terhune CE. 2010. The temporomandibular joint in anthropoid primates: functional, allometric, and phylogenetic influence. PhD Dissertation, Arizona State University.

Terhune CE. 2011a. Dietary correlates of temporomandibular joint morphology in New World primates. J Hum Evol 61:583–596.

Terhune CE. 2011b. Modeling the biomechanics of articular eminence function in anthropoid primates. J Anat 219:551–564.

Terhune CE. 2013. Dietary correlates of temporomandibular joint morphology in the great apes. Am J Phys Anthropol 150: 260–272.

Terhune CE, Hylander W, Vinyard C, Taylor A. 2011. Masseter fiber length and position influence relative maximum jaw gapes in the sexually-dimorphic *Macaca fascicularis*. Am J Phys Anthropol 144:292.

Terhune CE, Iriarte-Diaz J, Taylor AB, Ross CF. 2011. The instantaneous center of rotation of the mandible in nonhuman primates. Int Comp Biol 51:320–332.

Tomblin DC, Cranford JA. 1994. Ecological niche differences between Alouatta palliata and *Cebus capucinus* comparing feeding modes, branch use, and diet. Primates 35:265–274.

Ungar PS, M'Kirera F. 2003. A solution to the worn tooth conundrum in primate functional anatomy. Proc Natl Acad Sci USA 100:3874–3877.

Ungar PS, Williamson ME. 2000. Exploring the effects of tooth wear on function: a preliminary study of dental topography in *Gorilla gorilla*. Palaeont Electron 3:18.

van Roosmalen MGM, Mittermeier RA, Fleagle JG. 1988. Diet of the northern bearded saki (*Chiropotes satanas chiropotes)*: a neotropical seed predator. Am J Primatol 14:11–35.

Vinyard CJ. 1999. Temporomandibular joint morphology and function in strepsirrhine and eocene primates. PhD Dissertation, Northwestern University.

Vinyard CJ, Wall CE, Williams SH, Hylander WL. 2003. Comparative functional analysis of skull morphology of tree-gouging primates. Am J Phys Anthropol 120:153–170.

Wall CE. 1995. Form and function of the temporomandibular joint in anthropoid primates. PhD Dissertation, State University of New York at Stony Brook.

Wall CE. 1999. A model of temporomandibular joint function in anthropoid primates based on condylar movements during mastication. Am J Phys Anthropol 109:67–88.

Wall CE, Vinyard CJ, Johnson KR, Williams SH, Hylander WL. 2006. Phase II jaw movements and masseter muscle activity during chewing in *Papio anubis*. Am J Phys Anthropol 129:215–224.

Ward SC, Molnar S. 1980. Experimental stress analysis of topographic diversity in early hominid gnathic morphology. Am J Phys Anthropol 53:383–395.

Wiley DF, Amenta N, Alcantara DA, Ghosh D, Kil YJ, Delson E, Harcourt-Smith W, Rohlf FJ, St. John K, Hamann B. 2005. Evolutionary morphing. Proc IEEE Visualiz 2005.

Williams SH, Vinyard CJ, Wall CE, Hylander WL. 2007. Masticatory motor patterns in ungulates: a quantitative assessment of jaw-muscle coordination in goats, alpacas and horses. J Expir Zool A Ecolog Gen Physiol 307A:226–240.

Williams SH, Vinyard CJ, Wall CE, Hylander WL. 2009. Mandibular corpus bone strain in goats and alpacas: implications for understanding the biomechanics of mandibular form in selenodont artiodactyls. J Anat 214:65–78.

Winchester JM, Boyer DM, St. Clair EM, Gosselin-Ildari AD, Cooke SB, Ledogar JA. 2014. Dental topography of platyrrhines and prosimians: convergence and contrasts. Am J Phys Anthropol 153: 29–44.

Wright BW. 2005. Craniodental biomechanics and dietary toughness in the genus *Cebus*. J Hum Evol 48:473–492.

Wright PC. 1989. The nocturnal primate niche in the New World. J Hum Evol 18:635–658.